Chapter 4
Poincaré Plot in Capturing Nonlinear Temporal Dynamics of HRV

Abstract The method and importance of capturing temporal variation using standard descriptors (*SD1* and *SD2*) of Poincaré plot have been presented in Chap. 2. However, this does not include the temporal variation at point-to-point level of the plot. In addition, *SD1* and *SD2* descriptors are linear statistics (Brennan et al., IEEE Trans. Biomed. Eng. **48**:1342–1347, 2001) and hence the measures do not directly quantify the nonlinear temporal variations in the time series contained in the Poincaré plot. Although *SD1*/*SD2* is considered as a nonlinear measure, it yields mixed results when applied to the data sets that form multiple clusters in a Poincaré plot due to complex dynamic behaviours (Brennan et al., IEEE Trans. Biomed. Eng. **48**:1342–1347, 2001). This is because the technique relies on the existence of a single cluster or a defined pattern (Christopher et al., Biophys. J. **82**:206–214, 2002; Schechtman et al., Pediatr. Res. **40**:571–577, 1996). Therefore, further studies are required in defining new descriptors for analysing temporal variability of time series using Poincaré plots. Another driving force behind this study is the fact that the visual pattern of the Poincaré plot of heart rate variability signals relies upon clinical scenarios and the application of the existing standard descriptors in various studies has resulted in limited success.

4.1 Introduction

The method and importance of capturing temporal variation using standard descriptors (*SD1* and *SD2*) of Poincaré plot have been presented in Chap. 2. However, this does not include the temporal variation at point-to-point level of the plot. In addition, *SD1* and *SD2* descriptors are linear statistics [112] and hence the measures do not directly quantify the nonlinear temporal variations in the time series contained in the Poincaré plot. Although *SD1*/*SD2* is considered as a nonlinear measure, it yields mixed results when applied to the data sets that form multiple clusters in a Poincaré plot due to complex dynamic behaviours [112]. This is because the technique relies on the existence of a single cluster or a defined

A.H. Khandoker et al., *Poincaré Plot Methods for Heart Rate Variability Analysis*,
DOI 10.1007/978-1-4614-7375-6_4,

pattern [128,129]. Therefore, further studies are required in defining new descriptors for analysing temporal variability of time series using Poincaré plots. Another driving force behind this study is the fact that the visual pattern of the Poincaré plot of heart rate variability signals relies upon clinical scenarios and the application of the existing standard descriptors in various studies has resulted in limited success.

The inherent assumption behind using consecutive RR points in Poincaré plot is that the "present-RR-interval" significantly influences the "following-RR-interval". Various researchers reported that varying lags of Poincaré plot give better understanding about the autonomic control of the heart rate that influence the short-term and long-term variability of the heart rate [57,91]. A system can have different short- and long-term correlations on different time scales. When the sampling interval is less than the short-time correlation length, then these short-time correlations can be predominantly seen [130]. So in the context of short- or long-term variability, any point can influence at least a few successive points. Lerma et al. [131] reported that the current RR interval can influence up to approximately eight subsequent RR intervals in the context of the short-term variability. In another study, Thakre and Smith examined the theoretical demand with different lags and showed that there is a curvilinear relationship between lag Poincaré plot indices for normal subjects, which is lost in congestive heart failure (CHF) patients [132]. The relation between *lag*s and width of Poincaré plot (*SD1*) has been reported by Goshvarpour et al. [133]. Therefore, measurement from a series of lagged Poincaré plots (multiple lag correlation) can potentially provide more information about the behaviour of the underlying system than the conventional *lag-1* plot measurements [131].

The hypothesis of this chapter is that any descriptor that captures temporal information and is a function of multiple lag correlation, would provide more insight into the system rather than conventional measurements of variability of Poincaré plot (*SD1* and *SD2*), which are parameters of a *lag-1* correlation. In order to test this hypothesis, we propose a novel descriptor, complex correlation measure (*CCM*), for Poincaré plot that can be applied to measure the temporal variation of the Poincaré plot and is a function of multiple lag correlation of the signal.

4.2 Nonlinear Dynamics

4.3 Limitation of Standard Descriptors of Poincaré Plot

SD1 and *SD2* represent the distribution of the signal in 2D space and carry only spatial (shape) information. It should be noted that many possible RR interval series result in identical plot with exactly similar *SD1* and *SD2* values irrespective of different temporal structures. For example, two signals with similar *SD1* and *SD2* values, top panels (Fig. 4.1), are different in terms of temporal structure, bottom panels (Fig. 4.1).

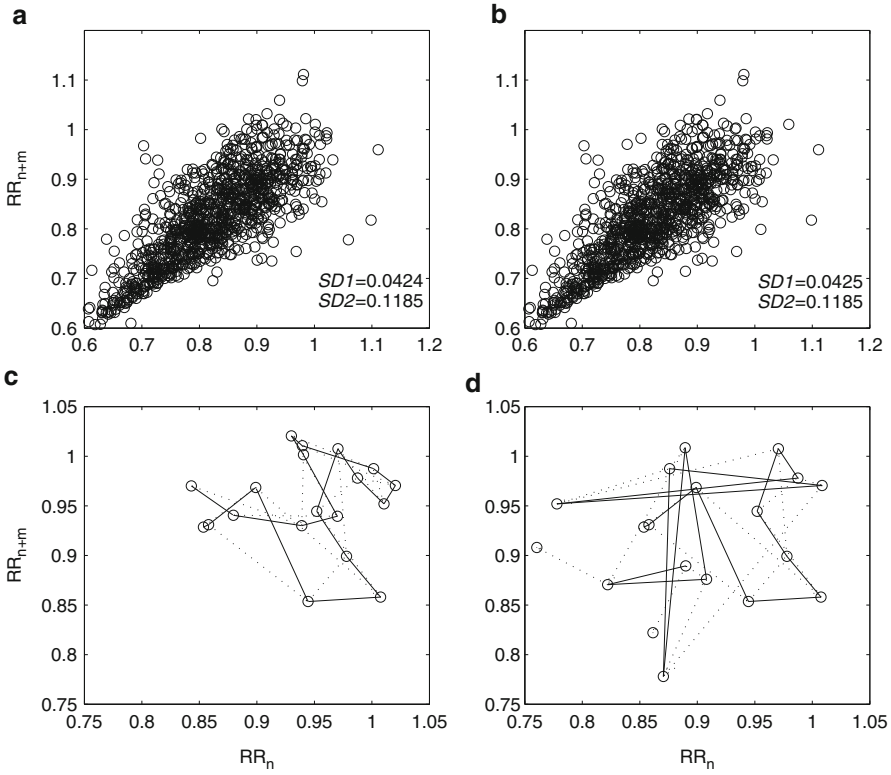

Fig. 4.1 Two different time series of length N ($N = 1,000$) with similar *SD1* and *SD2* values are shown ($m = 2$) on *top panel* (**a** and **b**). In the *bottom panel* (**c** and **d**) the underlying dynamics of first 20 points of both time series are shown to be different

Lerma et al. have shown that the measurement from a multiple lag Poincaré plot provides more information than any measure from single lag Poincaré plot [131]. Indeed, the Poincaré plot at any *lag-m* is more of a generalized scenario, where other levels of temporal variation of the dynamic system are hidden. As shown in equation sets 2.14 and 2.15, for any m, the descriptors *SD1* and *SD2* only indicate m lag correlation information of the plot. This essentially conveys overall behaviour of the system neglecting its detail temporal variation. The Poincaré plot of RR interval time series for three different lags is shown in Fig. 4.2. From the plots, it is obvious that for any time-series signal, different lag plots better reveal the behaviour of the signal than the single lag plot. The *CCM* is not only related to the *SD1* and *SD2*, but it also provides temporal information, which can be used to quantify the temporal dynamics of the system.

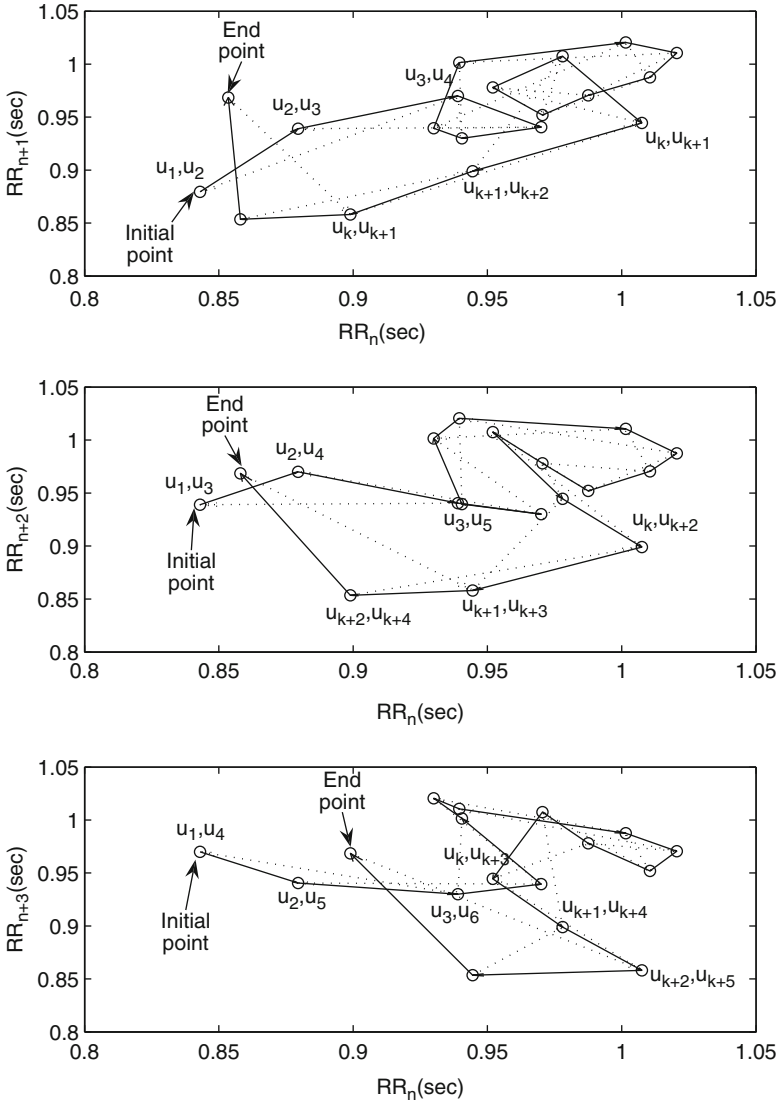

Fig. 4.2 Sequence of points (RR_n, $RR_{n+\tau}$) plotted and the *triangle* formed by each consecutive three points. Here, $m = \{1, 2, 3\}$ and $RR \equiv \{u_1, u_2, \ldots\ldots, u_N\}$.

4.4 Complex Correlation Measures in Poincaré Plot: A Novel Nonlinear Descriptor

The proposed descriptor *CCM* is computed using a moving window which embeds the temporal information of the signal. This moving window is comprised of three consecutive points from the Poincaré plot and the area of the triangle formed by

these three points is computed. This area measures the temporal variation of the points in the window. If three points are aligned on a line then the area is zero, which represents the linear alignment of the points. Moreover, since the individual measure involves three points of the two-dimensional plot, it is comprised of at least four different points of the time series for lag $m = 1$ and at most six points in case of lag $m \geq 3$. Hence the measure conveys information about four different lag correlations of the signal. Now, suppose the ith moving window is comprised of points $a(x1, y1)$, $b(x2, y2)$ and $c(x3, y3)$ then the area of the triangle (A) for ith window can be computed using the following determinant:

$$A(i) = \frac{1}{2}\begin{vmatrix} x1 & y1 & 1 \\ x2 & y2 & 1 \\ x3 & y3 & 1 \end{vmatrix}, \tag{4.1}$$

where A is defined on the real line $\Re$ and

$$\begin{aligned} A(i) &= 0, \text{ if points } a, b \text{ and } c \text{ are on a straight line} \\ &> 0, \text{ counterclockwise orientation the points } a, b \text{ and } c \\ &< 0, \text{ clockwise orientation of the points } a, b \text{ and } c. \end{aligned}$$

If Poincaré plot is composed of N points then the temporal variation of the plot, termed as *CCM*, is composed of all overlapping three point windows and can be calculated as

$$CCM(m) = \frac{1}{C_n(N-2)} \sum_{i=1}^{N-2} \|A(i)\|, \tag{4.2}$$

where m represents lag of Poincaré plot and C_n is the normalizing constant which is defined as $C_n = \pi * SD1 * SD2$ and represents the area of the fitted ellipse over Poincaré plot. The lengths of major and minor axis of the ellipse are $2SD1$ and $2SD2$.

Let the RR time series be composed of N RR interval values and defined as $RR \equiv u_1, u_2, \ldots, u_N$. As shown in Fig. 4.2, the *lag-1* Poincaré plot consists of $N-1$ numbers of 2D set of points PP, where $PP \in \{\Re, \Re\}$ can be represented by $PP \equiv \{(u_1, u_2), (u_2, u_3), \ldots, (u_{N-1}, u_N)\}$ and similarly for lag of m, $N-m$ numbers of 2D points are expressed as

$$PP \equiv \{(u_1, u_1+m), (u_2, u_2+m), \ldots, (u_{N-m}, u_N)\}.$$

Hence, for *lag-m* Poincaré plot, the first window will be composed of points $\{(u_1, u_{1+m}), (u_2, u_{2+m}), (u_3, u_{3+m})\}$ and from Eq. 4.1, the area A can be calculated as

$$A(1) = \frac{1}{2}[u_1u_{2+m} - u_1u_{3+m} + u_3u_{1+m} - u_2u_{1+m} + u_2u_{3+m} - u_3u_{2+m}]. \tag{4.3}$$

Similarly the second and $(N-m-2)$th window is composed of points $\{(u_2, u_{2+m}), (u_3, u_{3+m}), (u_4, u_{4+m})\}$ and $\{(u_{N-m-2}, u_{N-2}), (u_{N-m-1}, u_{N-1}), (u_{N-m}, u_N)\}$ respectively. Hence, the area, A, for second and $(N-m-2)$th window can be calculated as

$$\begin{aligned} A(2) = \frac{1}{2}[&u_2u_{3+m} - u_2u_{4+m} + u_4u_{2+m} - u_3u_{2+m} \\ &+u_3u_{4+m} - u_4u_{3+m}] \end{aligned} \tag{4.4}$$

$$\begin{aligned} A(N-m-2) = \frac{1}{2}[&u_{N-m-2}u_{N-1} - u_{N-m-2}u_N + u_{N-m}u_{N-2} \\ &-u_{N-m-1}u_{N-2} + u_{N-m-1}u_N - u_{N-m}u_{N-1}]. \end{aligned} \tag{4.5}$$

Using Eqs. 4.2–4.5, $CCM(m)$ is calculated as follows:

$$\begin{aligned} CCM(m) = \frac{1}{2C_n(N-2)} \Bigg[&u_{N-m}u_{N-1} + u_2u_{1+m} - u_{N-1-m}u_N - u_1u_{2+m} + \sum_{i=3}^{N-m} u_iu_{i-2+m} \\ &-2\sum_{i=2}^{N-m} u_iu_{i-1+m} + 2\sum_{i=1}^{N-1-m} u_iu_{i+1+m} - \sum_{i=1}^{N-2-m} u_iu_{i+2+m} \Bigg]. \end{aligned} \tag{4.6}$$

Since RR intervals are discrete signal, the autocorrelation at lag $m = j$ can be calculated as

$$\gamma_{RR}(j) = \sum_{n=1}^{N} RR_nRR_{n+j}. \tag{4.7}$$

Using Eqs. 2.14, 2.15, 4.6 and 4.7, $CCM(m)$ can now be expressed as a function of autocorrelation at different lags. Hence,

$$CCM(m) = F\left[\gamma_{RR}(0), \gamma_{RR}(m-2), \gamma_{RR}(m-1), \gamma_{RR}(m+1), \gamma_{RR}(m+2)\right]. \tag{4.8}$$

In the Eq. 4.8, $CCM(m)$ represents the point-to-point variation of the Poincaré plot with *lag-m* as a function of autocorrelation of lags $0, m-2, m-1, m+1$ and $m+2$. This supports our hypothesis that *CCM* is measured using multiple lag correlation of the signal rather than single lag. For the conventional *lag-1* Poincaré plot $CCM(1)$ can be represented as

$$CCM(1) = F\left[\gamma_{RR}(-1), \gamma_{RR}(0), \gamma_{RR}(2), \gamma_{RR}(3)\right]. \tag{4.9}$$

4.5 Mathematical Analysis of *CCM*

The *CCM* has been mathematically defined and its relation with multiple lag correlation information of the signal has been presented in the previous section. In this section, we explore the different properties of *CCM* with synthetic RR interval data.

4.5.1 Sensitivity Analysis

The sensitivity is defined as the rate of change of the value due to the change in temporal structure of the signal. The change in temporal structure of the signal in a window is achieved by surrogating the signal (i.e. data points) in that window. Sensitivity analysis of *CCM* will reveal the minimum length of the signal required to obtain a consistent *CCM* value. From the mathematical definition of *CCM*, we anticipated that *CCM* would be more sensitive to changes in temporal structure within the signal than the standard descriptors. We have compared the sensitivity of *CCM* with standard descriptors (*SD1*, *SD2*) in order to validate our assumption. A synthetic RR interval (*rr02*) time-series data from the open-access Physionet database [134] is used to validate the sensitivity analysis.

4.5.1.1 Sensitivity to Changes in Window Length

The sensitivity of *CCM* with different window lengths was analysed in order to define how it was affected by increasing the amount of change in temporal structure. The minimum number of samples required for using *CCM* as a measurement tool can also be defined using this analysis. The sensitivity to changes in window length is measured by increasing the window length in each step, changing the temporal structure of that window using surrogation and then calculating the *CCM* of the changed signal. Increased window length effectively increases the number of surrogating points, which results in increased probability of the amount of change in temporal structure of the time-series signal. At each step the number of surrogated points is increased by 50. We calculated *SD1*, *SD2* and *CCM* of the RR interval signal by increasing the number of surrogating points at a time. For a selected window length, we have shuffled the points 30 times, to minimize impact of bias of randomization, and calculated all descriptors each time after shuffling. Finally the surrogated values of descriptors were taken as a mean of the calculated values.

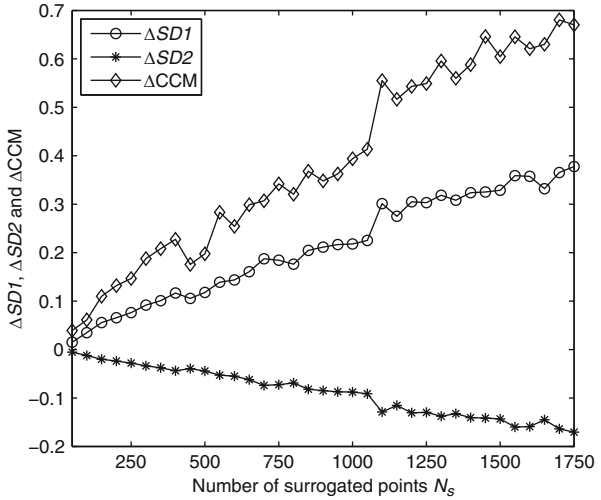

Fig. 4.3 Sensitivity of *SD1*, *SD2* and *CCM* with number of shuffled points N_s. At each step the number of shuffled points increased by 50. Each time the signal has been shuffled for 30 times and its mean has been taken to calculated the sensitivity

Then the sensitivity of descriptors $\Delta SD1_j$, $\Delta SD2_j$ and ΔCCM_j was calculated using Eqs. 4.10–4.12:

$$\Delta SD1_j = \frac{SD1_j - SD1_0}{SD1_0} \tag{4.10}$$

$$\Delta SD2_j = \frac{SD2_j - SD2_0}{SD2_0} \tag{4.11}$$

$$\Delta CCM_j = \frac{CCM_j - CCM_0}{CCM_0}, \tag{4.12}$$

where $SD1_0 = 0.36$, $SD2_0 = 0.08$ and $CCM_0 = 0.16$ were the parameters measured for the original data set without surrogation and j represents the window number whose data were surrogated and where, $SD1_j$, $SD2_j$ and CCM_j represent the *SD1*, *SD2* and *CCM* values, respectively, after surrogation of jth step.

The change of descriptors *SD1*, *SD2* and *CCM* with increasing number of shuffled RR intervals is presented in Fig. 4.3. From Fig. 4.3 it is obvious that the rate of change with number of shuffled RR intervals was higher for *CCM* at any point than *SD1* and *SD2*. Therefore, we can conclude that *CCM* is more sensitive than *SD1* and *SD2* with respect to change in temporal structure or the change in autocorrelation of the signal which was earlier reported by Karmakar et al. [135]. Moreover, sensitivity of *CCM* with small number of RR intervals increases its applicability to short-length HRV signal analysis.

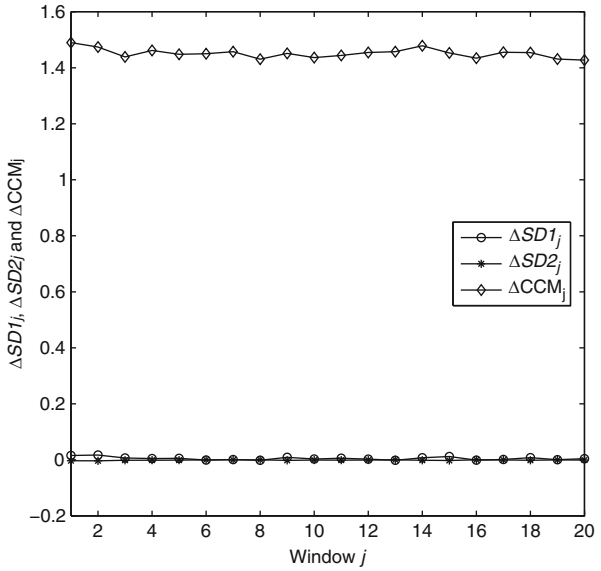

Fig. 4.4 Rate of change of values of *SD1*, *SD2* and *CCM* with surrogated data points within a window j over the whole data set

4.5.1.2 Homogeneity to Changes in Temporal Structure

In order to observe the homogeneity of sensitivity of *CCM* with changes in temporal structure over the whole timeline of the signal, we have used a fixed-length moving window, changed the temporal structure of that window using surrogation and then calculated *CCM* value of the changed signal. We have divided the signal into 20 windows with 200 samples in each of them. To minimize the bias from surrogated values, we have shuffled the points of each window 30 times and calculated all descriptors each time after shuffling. Finally, the surrogated values of descriptors were taken as a mean of the calculated values. Since we divided the entire signal into 20 windows, it resulted in 20 values of *SD1*, *SD2* and *CCM*. The sensitivity of descriptors $\Delta SD1_j$, $\Delta SD2_j$ and ΔCCM_j was calculated using Eqs. 4.10–4.12. Similar to the previous section, $SD1_0$, $SD2_0$ and CCM_0 were the parameters measured for the original data set without surrogation and j represents the window number whose data were surrogated.

Value of ΔCCM is significantly higher than $\Delta SD1$ and $\Delta SD2$ which indicates that *CCM* is much more sensitive than *SD1* and *SD2* to the underlying temporal structure of the data (Fig. 4.4). This supports the mathematical definition of *CCM* as a sensitive measure of temporal variation of the signal. The little variation in ΔCCM value shows that different temporal position of changes in temporal structure does not impact the *CCM* value, which means the homogeneity of *CCM* over time. Hence, *CCM* reflects changes in temporal structure of the signal irrespective of the time.

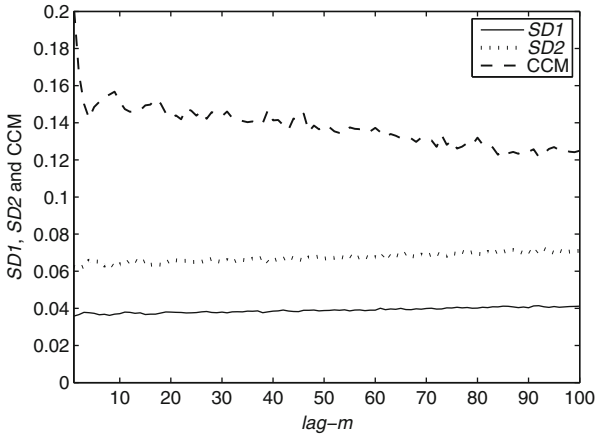

Fig. 4.5 Values of *SD1*, *SD2* and *CCM* for different *lag-m*

4.5.1.3 Examining the Influence of Various *lag*s of Poincaré Plot

One of the variations commonly used in order to optimize the use of the Poincaré plot as a quantitative tool is the lagged Poincaré plot [112, 136]. In several studies, it is also reported that the use of quantitative tool on multiple lagged Poincaré plot might be useful to distinguish normal from pathological heart rate signal [131, 132, 136]. Therefore, analysis of lag response might give a comprehensive idea about the use of *CCM*, as a new quantitative tool, in different physiological conditions.

To quantify the influence of various lags of Poincaré plot on *SD1*, *SD2* and *CCM*, values of all descriptors were calculated for different time delays or lags (*m* was varied in increments from 1 to 100). At each step, *lag-m* Poincaré plot was constructed and then *SD1*, *SD2* and *CCM* values were calculated for the plot.

The relationship of *CCM*, *SD1* and *SD2* with different lags (*m* was varied from 1 to 100) is shown in Fig. 4.5. A unit lag is used to create the Poincaré plot which confirms the maximum linear correlation among data points. This lag selection may have obscured the low-level nonlinearities of the signal and as a result *CCM* may be unable to show better performance over standard poincaré descriptors. In contrast, at higher lags, the standard descriptors are unable to capture the system dynamics. It is also established in the literature that studying behaviour of descriptors as a function of lags is more informative [132]. In our analysis, we have found that over different lags, *CCM* shows more variability than *SD1* and *SD2*. Among the three descriptors the change in values for *CCM* was higher than both *SD1* and *SD2* which again supports our claim of sensitivity of *CCM* with signal dynamics. Hence, we conclude that the change in underlying temporal structure due to lag of the Poincaré plot has higher impact on *CCM* than the traditional descriptors.

4.6 Physiological Relevance of *CCM* with Cardiovascular System

In this chapter, we demonstrate the physiological significance of the novel measure *CCM* by analysing the effects of perturbations of autonomic function on Poincaré plot descriptors (*SD1* and *SD2*) in HRV signal of young healthy human subjects caused by the 70° head-up tilt test, atropine infusion and transdermal scopolamine patch administration. A surrogate analysis is also performed on the data to show that changes found in different phases of the activity are due to perturbed autonomic activity rather than noise.

4.6.1 Subjects and Study Design

In this analysis, five subjects were studied with normal sinus rhythm, who did not smoke, had no cardiovascular abnormalities and were not taking any medications. Subjects were aged between 20 and 40 years (30.2 ± 7.2 years). All studies were performed at the same time of the day without any disturbances. No respiration control was performed because all phases of the study were conducted in the resting state. An intravenous cannula was inserted into an antecubital vein and subjects then rested 20 min before commencement of data collection. The length of the study varied from 10 to 20 min. For autonomic perturbations the following sequence of protocol was performed. At least 20 min was allowed between each phase to permit the heart rate to return to baseline. Details of the study design and data collection were published in [94]. The sequence of phases was maintained strictly as follows:

Baseline Study

All baseline studies were conducted in subjects in the post-absorptive state after resting for 10 min in the supine position.

Seventy Degree Head-Up Tilt

Data were collected after subjects were tilted 70° on a motorized table. This manoeuvre increases sympathetic and decreases parasympathetic nervous system activity [137]. To permit the heart rate to stabilize at new position, data were collected 5 min after the subjects were tilted.

Atropine Infusion

Atropine sulphate (1.2 mg) was added to 50 ml of 5 intravenous dextrose and infused at a rate of 0.12 mg/min for 5 min and then at a rate of 0.24 mg/min until completion of this phase of study. Use of this dose regimen reduces parasympathetic nervous system activity significantly [138]. After 10 min of infusion of atropine, the data collection started.

Transdermal Scopolamine

One week after the above studies, a low-dose transdermal scopolamine patch (hyoscine 1.5 mg) was applied overnight to an undamaged hair-free area of the skin behind the ear. The patch remained in situ for the duration of this period of the study. La Rovere et al. have shown that low-dose transdermal scopolamine increases parasympathetic nervous system activity [139].

4.6.2 Results

The RR intervals and the corresponding Poincaré plot for all four phases of the experiment with the same subject are shown in Fig. 4.6. From Fig. 4.6 it is eminent that the atropine infusion strongly reduces the size of plot by reducing both the RR interval (increase in heart rate) and its variation. Whereas, the head-up tilt position reduces the RR interval (increase in heart rate) variability markedly with respect to the baseline. In contrast, use of low-dose transdermal scopolamine increases the RR interval (reduces heart rate) and its variability resulted into a wider Poincaré plot in terms of width in both directions (perpendicular to line of identity and along the line of identity).

The mean and standard deviation of heart rate variability features of all subjects in all four phases are summarized in Table 4.1. Short-term variability (*SD1*) was increased in scopolamine phase and decreased in atropine phase. A similar trend was also found for long-term variability (*SD2*). Changes of *SD1* values from phase to phase were much higher than that of *SD2*. *CCM* value was also minimum in atropine phase and maximum at scopolamine phase. Changes in mean values of *CCM* between study phases were higher than both *SD1* and *SD2* (Table 4.1). Moreover, changes in *CCM* values in atropine, 70° head-up tilt and scopolamine phases from baseline are found significant ($p < 0.01$). Whereas, *SD1* values were significantly different in atropine and 70° Head-up tilt phases and *SD2* values only in atropine phase.

The errorbars of log-scaled *SD1*, *SD2* and *CCM* values for four groups of subjects are shown in Fig. 4.7. The atropine administration resulted into reduction in mean value of *SD1* (*SD* of ΔRR) all subjects which was also reported by Kamen et al. [94]. The similar effect was also found for *SD2* and *CCM*. The use of scopolamine patch increased both the width and height of the Poincaré plot which resulted in the

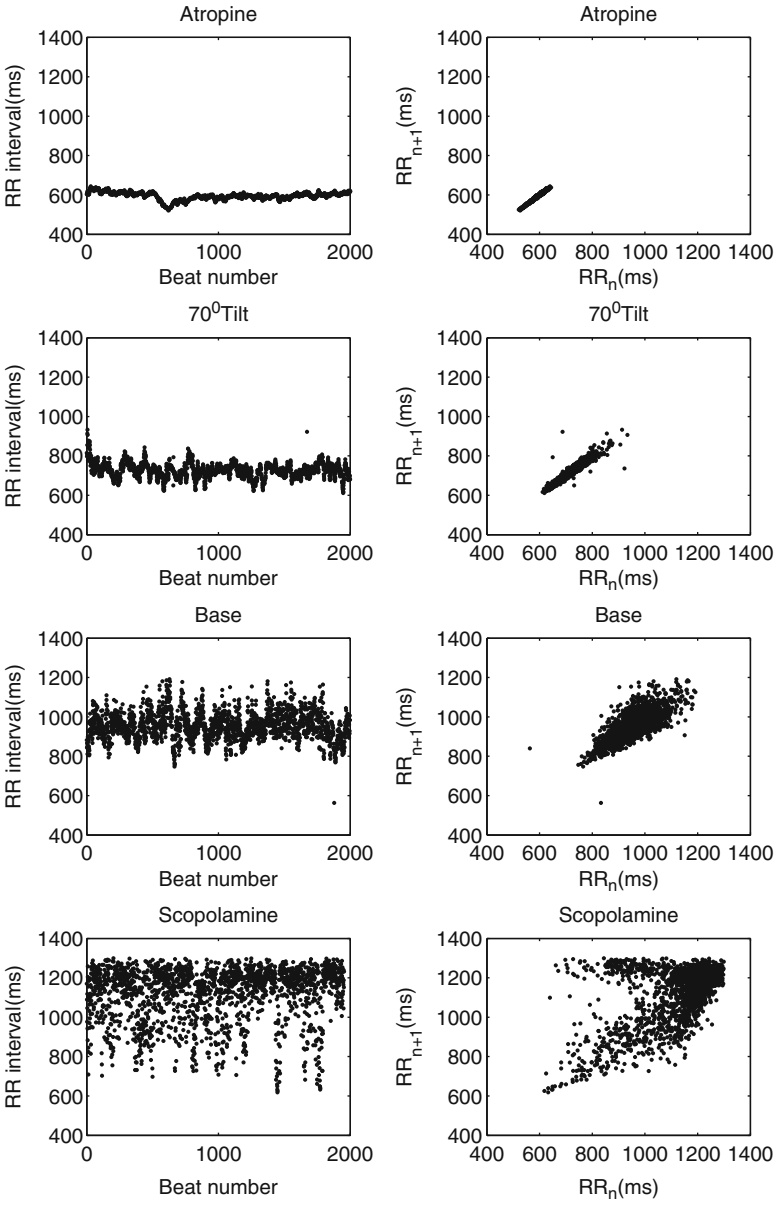

Fig. 4.6 RR interval time series for single subject from all four phases of study with corresponding Poincaré plot

Table 4.1 *Mean* and standard deviation *SD* of values of all descriptors for *lag-1* Poincaré plot

Feature	*SD1* (mean ± sd) (ms)	*SD2* (mean ± sd) (ms)	*CCM* (mean ± sd)
Atropine	4.45 ± 2.45*	43.11 ± 13.79*	3.88E-02 ± 1.05E−02*
Head-up tilt	11.96 ± 5.47	70.77 ± 13.98	6.29E-02 ± 2.08E−02*
Baseline	28.74 ± 9.28	85.94 ± 11.27	1.50E-01 ± 3.40E-02
Scopolamine	69.90 ± 21.25*	103.05 ± 20.05	2.75E-01 ± 2.14E−02*

SD1, *SD2* and *CCM* values of all subjects ($N = 5$) were calculated for four phases as described in Sect. 4.6.1. * indicates the value of the feature in corresponding phase is significantly ($p < 0.01$) different from baseline phase using Wilcoxon rank-sum test

increase in mean values of *CCM* as well as *SD1* and *SD2*. All subjects have shown a marked reduction in *SD1*, *SD2* and *CCM* values in 70° head-up tilt phase compared to the baseline.

4.6.3 Physiological Relevance of CCM

Quantitative Poincaré plot analysis was used to assess the changes in HRV during parasympathetic blockade [111] and compared the results with power spectral analysis of HRV, which was the commonly used method in the measurement of sympathovagal interaction [13, 103, 111, 140]. It was also reported that Poincaré analysis method can provide the heart rate dynamics that is not detected by the conventional time-domain methods [111]. The present quantitative analysis was performed to measure the instantaneous beat-to-beat variance of RR intervals (*SD1*), the long-term continuous variance of all RR intervals (*SD2*) and the variation in temporal structure of all RR intervals (*CCM*). Instantaneous changes in RR intervals are mediated by vagal efferent activity, because vagal effects on the sinus node are known to develop faster than sympathetically mediated effects [101, 124]. The maximum reduction in *SD1* during atropine infusion compared to baseline values confirms that *SD1* quantifies the vagal modulation of heart rate, which was also reported by Kamen et al. [94] and Tulppo et al. [111]. Similar reduction in *CCM* value could be observed (Table 4.1 and Fig. 4.7), which indicates that *CCM* might correlate the parasympathetic nervous system activity. The lowest value of *CCM* has also been found during atropine infusion which reduced the parasympathetic activity and reduces instantaneous changes in HRV signal. Moreover, significant ($p < 0.01$) change in *CCM* values in all phases from baseline phase compared to *SD1* and *SD2* indicates that *CCM* is more sensitive to changes in parasympathetic activity (Table 4.1). On the contrary, changes in *SD1* values are insignificant in 70° head-up tilt phase and changes in *SD2* values are insignificant both in 70° head-up tilt and scopolamine phases.

Reciprocal changes in sympathetic and parasympathetic activity occur during head-up tilt phase. The RR interval decreases and the high-frequency power of RR intervals decreases during the head-up tilt phase as evidence of withdrawal

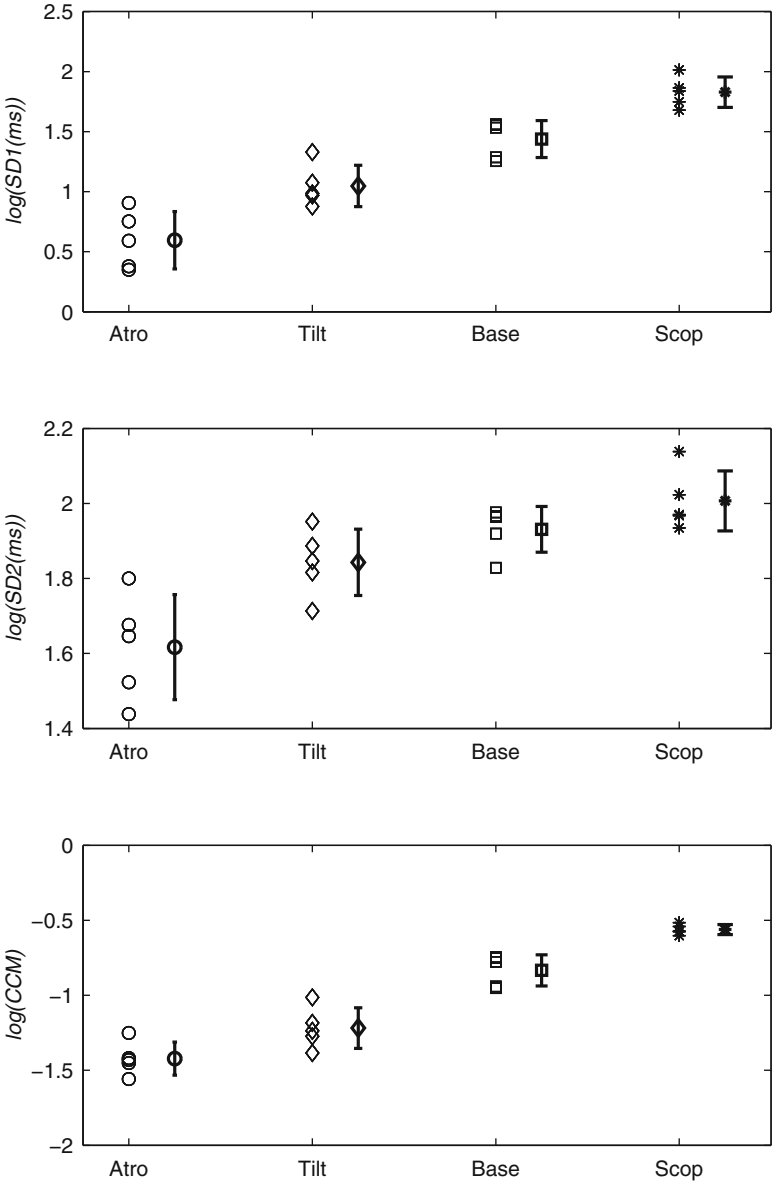

Fig. 4.7 Errorbar ($n = 5$) of $log(SD1)$, $log(SD2)$ and $log(CCM)$ for atropine (Atro), 70° head-up tilt (Tilt), baseline (Base) and scopolamine (Scop) phase. All values were calculated for short-segment (~ 20 min) RR interval time-series signal

of vagal activity (decrease in parasympathetic activity) [104, 141, 142]. The short-term variability measure of Poincaré plot (*SD1*) also decreases and correlates with high-frequency power as reported by Kamen et al. [94]. In this study, *SD1* value decreased during 70° head-up tilt phase compared to baseline, which supports the results reported by previous studies [94, 137]. The *CCM* value has also decreased in 70° head-up tilt phase compared to baseline, which indicates that *CCM* value is modulated by the vagal tone (parasympathetic activity). Therefore, changes in autonomic regulation caused by 70° head-up tilt phase resulted in concordant changes in the temporal structure of the Poincaré plot of RR intervals.

The low-dose transdermal scopolamine patch may decrease heart rate by a paradoxical vagomimetic effect [139]. Delivery by transdermal patch substantially increases both baseline and reflexly augmented levels of cardiac parasympathetic activity over 24 h in normal subjects [143, 144]. Both time-domain HRV (mean, SD) and frequency-domain HRV (high-frequency power) increased to a greater extent during administration of low-dose scopolamine, which indicates the increase in parasympathetic activity [139]. The increase in parasympathetic activity decreases the heart rate and increases the RR interval as well as instantaneous variance in the RR, as measured by *SD1* of Poincaré plot. The increased value of *SD1* correlates with increase high-frequency power and supported by the previous study reported by Kamen et al. [94]. In this study, the variability in the temporal structure of the Poincaré plot (measured as *CCM*) was also found to be increased with increase in parasympathetic activity during administration of low-dose scopolamine (Fig. 4.7, Table 4.1). The increase in *CCM* value indicates that it reflects the change in parasympathetic activity harmoniously.

4.7 Clinical Case Studies Using *CCM* of Poincaré Plot

In order to validate the proposed measure "*CCM*" two case studies were conducted on RR interval data. The data from MIT-BIH Physionet database are [145] used in the analysis. The medical fraternity has utilized Poincaré plot, using both qualitative and quantitative approaches, for detecting and monitoring arrhythmia. Compared to arrhythmia, fewer attempts have been made to utilize Poincaré plot to evaluate CHF. In this study, we have analysed the performance of *CCM* and compared it with that of *SD1* and *SD2* for recognizing both arrhythmia and CHF using HRV signals.

4.7.1 HRV Studies of Arrhythmia and Normal Sinus Rhythm

In this study, we have used 54 long-term ECG recordings of subjects in normal sinus rhythm (30 men, aged 28.5–76, and 24 women, aged 58–73) from Physionet Normal Sinus Rhythm database [145]. Furthermore, we have also used NHLBI-sponsored cardiac arrhythmia suppression trial (CAST) RR-Interval Sub-study database for the arrhythmia data set from Physionet. Subjects of CAST database had an acute

myocardial infarction (MI) within the preceding 2 years and 6 or more ventricular premature complexes (PVCs) per hour during a pre-treatment (qualifying) long-term ECG (Holter) recording. Those subjects enrolled within 90 days of the index MI were required to have left ventricular ejection fractions less than or equal to 55 %, while those enrolled after this 90 day window were required to have an ejection fraction less than or equal to 40 %.

The database is divided into three different study groups, among which we have used the Encainide (e) group data sets for our study. From that group we have chosen 272 subjects belonging to subgroup baseline (no medication). The original long-term ECG recordings were digitized at 128 Hz, and the beat annotations were obtained by automated analysis with manual review and correction [145]. *lag-1* Poincaré plots were constructed for both normal and arrhythmia subjects and the new measure *CCM* was computed along with *SD1* and *SD2*. The *SD1* and *SD2* were calculated to characterize the distribution of the plots, whereas *CCM* values were used for characterizing the temporal structure of the plots.

Figure 4.8a represents box-whiskers (BW) plot for $log(SD1)$ and it is obvious that boxes (interquartile range) of normal and arrhythmia subjects are non-overlapping. But the whiskers (upper quartile) of normal subjects completely overlap with the whiskers (lower quartile) of the arrhythmia subjects. In Fig. 4.8b, the BW plot of $log(SD2)$ is shown and it is apparent that the BW of normal subjects completely overlapped with the whiskers (lower quartile) of the arrhythmia subjects. But the box of arrhythmia subjects is still non-overlapping with the whiskers (upper quartile) of the normal subjects. In Fig. 4.8c, the BW plot of $log(CCM)$ is shown and it is obvious that both of them are non-overlapping and distinct.

The p values obtained from ANOVA analysis between two groups for *SD1*, *SD2* and *CCM* are given in Table 4.2. Using ANOVA, for *CCM*, $p = 6.28 \times 10^{-18}$ is obtained, whereas for *SD1* and *SD2*, it is 7.6×10^{-3} and 8.5×10^{-3}, respectively. In case of $p < 0.001$ to be considered as significant, only *CCM* would show the significant difference between two groups which indicates that *CCM* is a better descriptor of HRV signal than *SD1* and *SD2* when comparing arrhythmia with normal sinus rhythm subjects.

4.7.2 HRV Studies of Congestive Heart Failure and Normal Sinus Rhythm

For this case study, we have used 29 long-term ECG recordings of subjects (aged 34 to 79) with CHF (NYHA classes I, II and III) from Physionet CHF database along with 54 ECG recordings of subjects with normal sinus rhythm as discussed earlier [145]. The same ECG acquisition with beat annotations was used as discussed in the previous case study. Similar to the previous case study, *lag-1* Poincaré plots were constructed for both normal and CHF subjects and the new descriptor *CCM* was computed as per traditional descriptors.

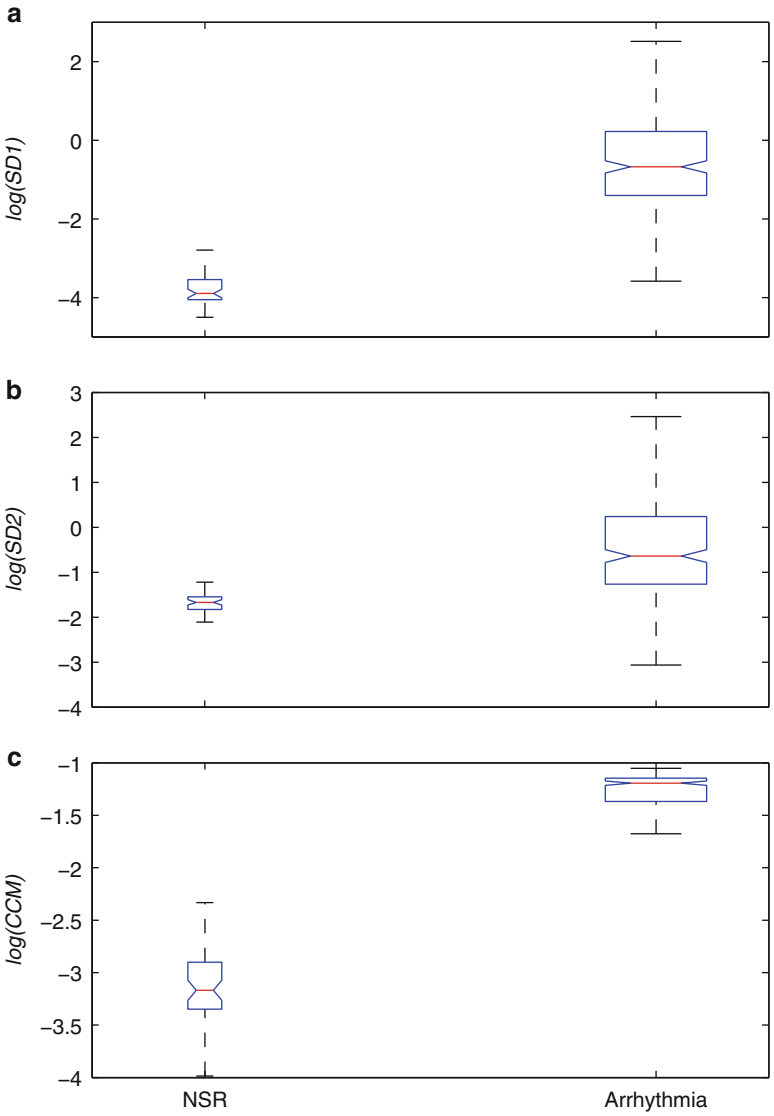

Fig. 4.8 Box-whiskers plot of (**a**) *SD1*, (**b**) *SD2* and (**c**) *CCM* for normal sinus rhythm (NSR, $n = 54$) and arrhythmia ($n = 272$) subjects

Figure 4.9a represents BW plot for $log(SD1)$ and it is apparent that boxes (interquartile range) of normal and CHF subjects are overlapping. The BW of normal subjects is completely overlapped with the box and whisker (lower quartile) of the CHF subjects. In Fig. 4.9b, the box-whiskers plot of $log(SD2)$ is shown and boxes are apparently non-overlapped. But the BW plot of normal subjects mostly

Table 4.2 *Mean* ± *standard deviation* of *SD1*, *SD2* and *CCM* for normal and arrhythmia subjects

	SD1	*SD2*	*CCM*
Normal	0.03 ± 0.02	0.19 ± 0.04	0.05 ± 0.03
arrhythmia	1.92 ± 5.18	2.30 ± 5.86	0.26 ± 0.08
p value (ANOVA)	7.60E−3	8.50E−3	6.28E−18

p values from ANOVA analysis are given in the last row

overlaps with the whisker (upper quartile) of the CHF subjects. In Fig. 4.9c, the BW plot of $log(CCM)$ is shown to be non-overlapping and only the upper quartile (box) and whisker of normal subjects are overlapped with the whisker (lower quartile) of the CHF subjects.

The values of the mean and the standard deviation for both types of subjects are shown in Table 4.3. Last row represents the p value obtained from ANOVA analysis between the two groups for *SD1*, *SD2* and *CCM*. Though *SD2* and *CCM* show similar difference between the mean of two subject groups, the *standard deviation* of *CCM* is lower which concentrates with the distribution of *CCM* values around mean comparing with that of *SD2*. The p value, obtained from ANOVA analysis for *CCM* ($p = 9.07 \times 10^{-14}$), shows more significance than *SD1* and *SD2*.

4.8 Critical Remarks on *CCM*

The main motivation for using Poincaré plot is to visualize the variability of any time-series signal. In addition to this qualitative approach, we propose a novel quantitative measure, *CCM*, to extract underlying temporal dynamics in a Poincaré plot. Surrogate analysis showed that the standard quantitative descriptors *SD1* and *SD2* were not as significantly altered as did *CCM*, this is shown in Fig. 4.3. Both *SD1* and *SD2* are second-order statistical measures [112], which are used to quantify the dispersion of the signal perpendicular and along the line of identity, respectively. Moreover, *SD1* and *SD2* are functions of *lag-m* correlation of the signal for any m lag Poincaré plot. In contrast, *CCM* is a function of multiple lag ($m-2$, $m-1$, m, $m+1$, $m+2$) correlations and hence, this measure was found to be sensitive to changes in temporal structure of the signal as shown in Fig. 4.3.

From the theoretical definition of *CCM* it is obvious that the correlation information measured in *SD1* and *SD2* is already present in *CCM*. But this does not mean that *CCM* is a derived measure from existing descriptors *SD1* and *SD2*. Rather, *CCM* can be considered as an additional measure incorporating information obtained in *SD1* and *SD2* (as the *lag-m* correlation is also included in *CCM* measure). In a Poincaré plot, it is expected that lag response is stronger at lower values of m and it attenuates with increasing values of m. This is due to the dependence of Poincaré descriptors on autocorrelation functions. The autocorrelation function monotonically decreases with increasing lags and in case of RR interval time series,

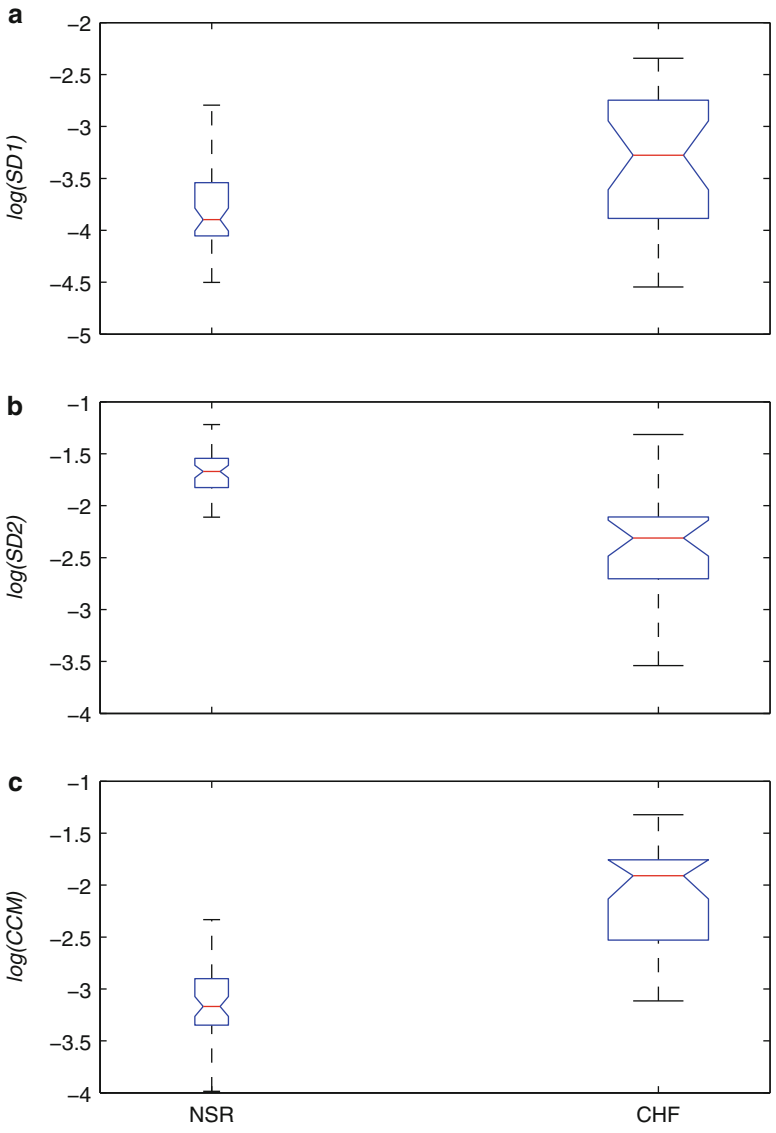

Fig. 4.9 Box-whiskers plot of (**a**) *SD1*, (**b**) *SD2* and (**c**) *CCM* for normal sinus rhythm (NSR, $n = 54$) and congestive heart failure (CHF, $n = 29$) subjects

usually the current beat influences only about six to eight successive beats [132]. In this study, we also found that all measured descriptors *SD1*, *SD2* and *CCM* changed rapidly at lower lags and the values are stabilized with higher lag values (Fig. 4.5). Since *CCM* is also a function of the signals autocorrelations, it shows a

Table 4.3 *Mean* ± *standard deviation* of *SD1*, *SD2* and *CCM* for normal and congestive heart failure (CHF) subjects

	SD1	*SD2*	*CCM*
Normal	0.03 ± 0.02	0.19 ± 0.04	0.05 ± 0.03
CHF	0.04 ± 0.02	0.11 ± 0.06	0.14 ± 0.06
p value (ANOVA)	5.65E−4	5.04E−12	9.07E−14

p values from ANOVA analysis are given in the last row

similar lag response to that shown by *SD1* and *SD2*. Therefore, *CCM* may be used to study the lag response behaviour of any pathological condition in comparison with normal subjects or controls.

HRV measure is considered to be a better marker for increased risk of arrhythmic events than any other non-invasive measure [146, 147]. An earlier study has shown that Poincaré plots exposed completely different 2D patterns in the case of arrhythmia subjects [148]. These abnormal medical conditions have complex patterns due to reduced autocorrelation of the RR intervals. Consequently due to the changes in autocorrelation, we have found that the variability measure using Poincaré (*SD1*, *SD2*) was higher than normal subjects (shown in Table 4.2). Moreover, the fluctuations of these variability measures were also very high in the case of arrhythmias. This may be due to different types of arrhythmia along with subjective variation of HRV. In arrhythmia subjects, *CCM* was found to be higher compared to NSR subjects, but the deviation due to subjective variation is much smaller than *SD1* and *SD2*. As a result, *CCM* linearly separates these two groups of subjects which means that the effect of different types of arrhythmia and subjective variation are reduced while using *CCM* than other variability measures. Therefore, we may conclude that *CCM* is a better marker for recognizing arrhythmia than the traditional variability measures of Poincaré plot.

In case study, we have also shown how the Poincaré plot can be used to characterize CHF subjects from normal subjects using RR interval time series. Compared to *SD2*, *SD1* and *CCM* values were found to be higher in CHF subjects. This finding might indicate that the short-term variation in HRV is higher in CHF subjects; however, the long-term variation is reduced. Since *CCM* captures the signal dynamics at short level (i.e, three points of the plot), it appears to be affected by short-term variation of the signal in CHF subjects. In the case of recognition of CHF subjects, although *SD2* showed good results, *CCM* was found to be more significant (Table 4.3).

So far the discussion indicates that *CCM* is an additional descriptor of Poincaré plot along with *SD1* and *SD2*. This also implies that *CCM* is a more consistent descriptor compared to *SD1* and *SD2*. Considering the presented case studies, it is clear that neither *SD1* nor *SD2* alone can independently distinguish NSR subjects from CHF and arrhythmia subjects. However, in the same scenario, *CCM* has the ability to perform the classification task independently. This justifies the usefulness of the proposed descriptors as a feature in a pattern recognition scenario. Our primary motivation for detecting pathology with a novel descriptor like *CCM*

rather than by observing a visual pattern is achieved, as shown by the case studies described. Although we have not looked at the physiological interpretation of *CCM*, the following remarks are relevant. The Poincaré plot reflects the autocorrelation structure through the visual pattern of the plot. The standard descriptors *SD1* and *SD2* summarize the correlation structure of RR interval data as shown by Brennan et al. [112]. *CCM* is based on the autocorrelation at different lags of the time series, hence giving an in-depth measurement of the correlation structure of the plot. Therefore, the value of *CCM* decreases with increased autocorrelation of the plot. In arrhythmia, the pattern of the Poincaré plots becomes more complex [148], thus reducing the correlation of the signal (RR_i, RR_{i+1}). In case of healthy subjects the value of *CCM* is lower than that of arrhythmic subjects. In the future, the performance of CCM for other pathologies might be worth looking.

4.9 Conclusion

CCM is developed based on the limitation of standard descriptors *SD1* and *SD2*. The analysis carried out confirms the hypothesis that *CCM* measures the temporal variation of the Poincaré plot. In contrast to the standard descriptors, *CCM* evaluates point-to-point variation of the signal instead of gross variability. *CCM* is more sensitive to changes in temporal variation of the signal and varies with different lags of Poincaré plot. Besides the mathematical definition of *CCM* and analysing properties of the measure, *CCM* was found to be effective in the assessment of different physiological and pathological conditions.